Atmospheric Mixed Layers over the South China Sea during SCSMEX

Paul E. Ciesielski and Richard H. Johnson
Department of Atmospheric Science, Colorado State University, Fort Collins, Colorado, USA

Abstract

Sounding data from the South China Sea Monsoon Experiment (SCSMEX) have provided a unique opportunity to document the variability of atmospheric mixed layers over the South China Sea (SCS) during the onset of the monsoon in this region. Six-hourly sounding data from two research vessels, deployed over the northern and southern SCS, are used to determine the mixed-layer depth and its thermodynamic properties.

Results from the southern ship show the presence of mixed layers 83% of the time with a mean depth of 459 m, similar to other tropical oceanic locations. On the other hand, the northern ship exhibited mixed layers 48% of the time with a mean depth of 342 m, considerably less frequent and shallower than other tropical regions. This anomalous behavior, which was particularly evident after the monsoon onset, is likely due to northward advection of low-level warm, moist air over cooler waters, which results in very small or negative buoyancy fluxes over the northern SCS, and thus weak upward mixing of heat and moisture from the surface.

1. Introduction

During the onset of the Southeast Asian Summer Monsoon (SEAM), convection establishes itself over Southern China and the northern SCS. With the ultimate goal of obtaining a comprehensive description of the SEAM to improve its predictability, SCSMEX was designed to investigate the processes associated with the monsoon onset and development during May and June, 1998. An important aspect of the monsoon in this region is the coupling between the ocean and the atmosphere. Since the atmospheric mixed layer (generally the lowest 0.5 km of the troposphere) is the medium through which the ocean and the free atmosphere are coupled, this study documents the properties and evolution of the mixed layer over the SCS during SCSMEX.

2. Data sources and procedure for determining mixed layers

During the SCSMEX intensive observing period (IOP) from 5 May to 22 June, two sounding networks (Fig. 1) were established over the SCS to determine and contrast the properties of convection in two distinct ocean regions of the SEAM. An integral part of these networks were two research vessels (R/Vs) which provided hourly surface fluxes in addition to four high-vertical resolution sondes per day. The northern sounding array was centered around the R/V Shiyan 3, which was nominally located at 20.4°N, 117°E. The R/V Kexue 1 was located on the perimeter of the southern array at 6.2°N, 110°E. Hereafter we shall refer to these sites as Ship 3 and Ship 1, respectively. These ships were on location for the entire IOP except for a 9-day port call near the end of May. Also shown in Fig. 1 is the SST analysis for this period based on the TRMM microwave imager (TMI) product (Wentz et al. 2000). The rainfall estimates used in this paper were obtained from the 3-h, 0.25° TRMM 3B42 version 6 TMI/IR merged rainfall product (Huffman et al. 2007). Surface fluxes were computed from ship observations and supplemented with fluxes from the Japan Meteorological Agency (JMA) Global Energy and Water cycle EXperiment (GEWEX) Asian Monsoon Experiment (GAME) V1.1 special reanalysis for the SCSMEX.

For the analysis in this study we used 5-hPa vertical resolution (1005, 1000 hPa, ect.) sounding data. Both sounding sites used Vaisala RS80 sondes. The overall data quality at these sites appeared to be quite good, although the humidity data likely contain a daytime dry bias (Cady-Pereira et al. 2008) that was not corrected here. However, as noted in Johnson et al. (2001; hereafter JCC01), this type of error will not alter the determination of the mixed-layer depth which relies on vertical gradient information.

In this study, a subjective technique, using both potential temperature (θ) and specific humidity (q) profiles, was used to identify mixed-layer tops. This technique was used to identify mixed layers over the western Pacific using sounding data from the Tropical Ocean Global Atmosphere Coupled Ocean-Atmosphere Experiment (TOGA COARE) as described in JCC01. Specifically, the mixed-layer top or inversion base (z_i) is identified as the level at which θ exhibits an abrupt increase with height (with a near constant value below) and q has a sharp decrease with height (following a slight decrease or constant value below). Both of these structures must be present for a sounding to be assigned a z_i. Details of this technique along with examples of the procedure can be found in JCC01. By using 5-hPa (~50 m) resolution data in this study, z_i can be determined to within ~50 m.

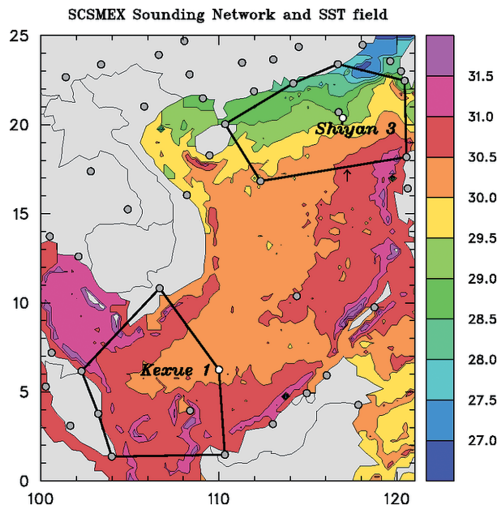

Fig. 1. Map of SCSMEX sounding network showing the location of sounding sites (gray circles with R/Vs denoted by white circles). Color shading shows the SST field for the SCSMEX IOP with scale to right.

Corresponding author: Paul E. Ciesielski, Department of Atmospheric Science, Colorado State University, Fort Collins, Colorado 80523, USA. E-mail: paulc@atmos.colostate.edu.

3. Mean properties of the mixed layer

The IOP-mean properties of the mixed layers for the two sites in question are listed in Table 1. The mean height for Ship 1 of 459 m is similar to what was observed in other tropical regions (424 m in GATE, 512 m in TOGA COARE, JCC01). The frequency of mixed layers at Ship 1 of 83% is somewhat higher than the 72% observed in TOGA COARE. On the other hand, the mean mixed-layer height and frequency for Ship 3 of 342 m and 48%, respectively, are considerably lower than that found in other tropical regions. The standard deviation of z_i at both sites is quite similar (~110 m) and considerably smaller than that observed in TOGA COARE (~155 m). The larger variability in COARE is likely related to the buildup and decay of westerly wind bursts (WWBs), occurring on intraseasonal time scales, during which convective conditions and associated processes affecting mixed-layer depth varied substantially. While convectively active and suppressed periods were observed during SCSMEX (see rainfall time series in Figs. 4 and 5), the range of conditions over the SCS was likely not as large as that observed in TOGA COARE.

The histograms of the mixed-layer tops for the two sites are shown in Fig. 2. The characteristics of the histogram for Ship 1 (namely, the higher mean and the normal shape of the distribution) are quite similar to those observed in TOGA COARE (JCC01). The prevalence of shallow mixed layers at Ship 3 results from a combination of factors including weaker buoyancy fluxes, heavier rainfall events and/or a higher frequency of shallow, recovering precipitation downdraft wakes near this site.

By scaling each profile by its mixed-layer depth in order to preserve the boundary layer structure, scaled-mean profiles of wind speed, θ, virtual potential temperature θ_v, and q at the two sites were computed (Fig. 3). The profiles of θ, θ_v and q are nearly well mixed from ~50m above the surface to ~50 m below z_i. While slightly unstable conditions are evident in θ_v profiles near the surface, these values may reflect some contamination from the ships' structure (denoted by shading in Fig. 3). Also, the sonde data (i.e., data points above the surface) have not been corrected for any solar heating effects, which may contribute to the jumps between the lowest sonde point and the surface data which comes from a measurement independent from the sonde.

The most obvious difference between the two sites, aside from the shallower mixed layers at Ship 3, is seen in the θ and θ_v profiles where the Ship 3 temperature profile is ~1°C cooler than that at Ship 1. This difference is likely a consequence of the local SST which is also ~1 °C cooler at Ship 3 (Fig. 1 and Table 1). Mixed-layer wind speeds are slightly stronger and moisture values slightly higher at Ship 3. The mixed-layer values of q at the SCSMEX ships (~19 g kg^{-1}) are ~8% higher than those observed in TOGA COARE (~17.5 g kg^{-1}) as noted in JCC01.

Table 1. Mean mixed-layer statistics averaged over both cruises. SSTs and rainfall rates are averaged in a circle with a 2° radius centered on ship locations.

Station	Ship 1	Ship 3
No. (percent)	126 (83%)	74 (48%)
Mean z_i (m)	459	342
σ (m)	113	111
z_i range (m)	162–728	140–645
LCL (m)	614	466
LCL – z_i (m)	156	124
SST (C)	30.6	29.5
rainfall (mm day^{-1})	4.7	9.4

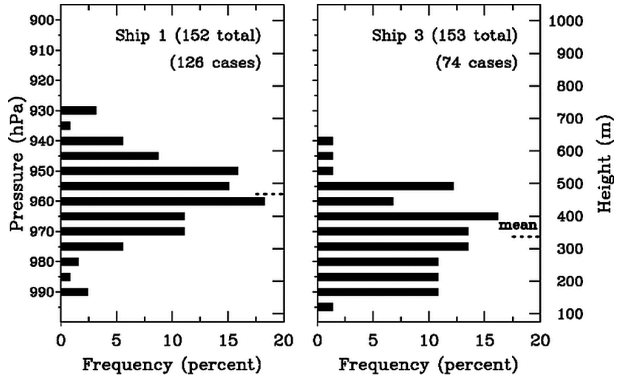

Fig. 2. Histograms for Ship 1 (left) and Ship 3 (right) showing the frequency of occurrence (percent) of a mixed layer top at a given pressure level (using 5-hPa resolution data). Mean mixed-layer depth is indicated with a short dashed line along the right axis of each panel.

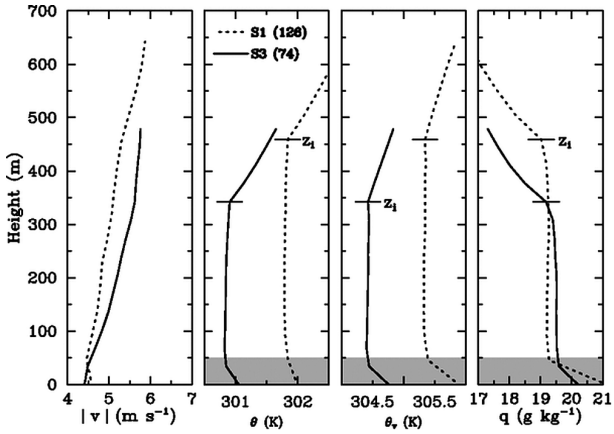

Fig. 3. Scaled mean mixed-layer profiles of wind speed (left panel), potential temperature (left-center panel), virtual potential temperature (right-center panel), and specific humidity (right panel) for ship sites in SCSMEX constructed using the number of sondes indicated in parentheses. S1 refers to Ship 1 and S3 to Ship 3. Mean values of mixed-layer depth are indicated with short solid horizontal lines intersecting various curves. Shaded regions in the lowest 50 m indicate questionable thermodynamic data in this layer.

4. Temporal variability of mixed layer

Time series of mixed-layer tops at Ship 1 and Ship 3 for the SCSMEX period are shown in Figs. 4 and 5, respectively. Also included in these figures are time series of SST and rainfall within a 2° radius of the ships; surface values of wind speed, relative humidity (RH), temperature (T_s), and buoyancy flux F; and estimated cloud base height (*CBH*). Here, F is defined as $F = S + 0.61 c_p T_s E/L$ where S is the sensible heat flux, E the latent heat flux, L the latent heat of vaporization, and c_p the specific heat of dry air. The surface fluxes were computed using the TOGA COARE bulk flux formula (Fairall et al. 1996) with measurements taken on the ships. When the ships were not on location, surface fluxes were estimated by using ship-adjusted JMA reanalysis values while other fields in these figures were obtained by interpolation to the ship locations from a

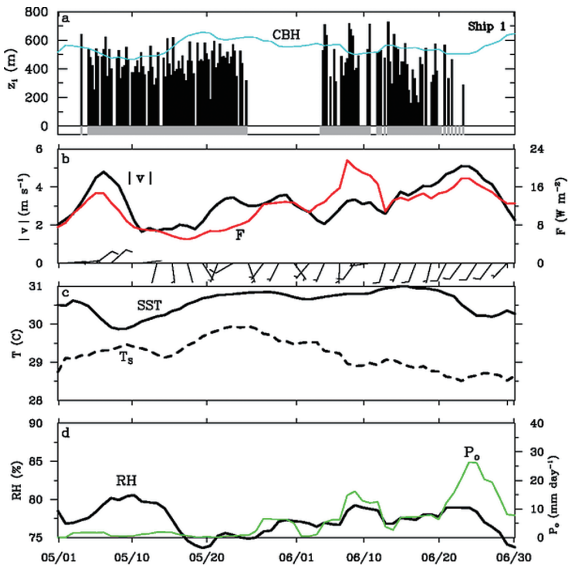

Fig. 4. Time series of various fields from Ship 1. Panel (a) shows mixed-layer tops (tops of vertical solid bars) and estimated cloud base height (cyan line) where dark-shaded regions at bottom of this panel indicate times at which soundings were taken; (panel b) surface wind speed (heavy line with scale to left), buoyancy flux (red line with scale to right) and surface wind barbs (with speed in knots); (panel c) T_s (dashed) and SST (solid); (panel d) surface RH (heavy line with scale to left) and rainfall (green line with scale to right). All fields except z_i have been filtered with a 5-day running mean.

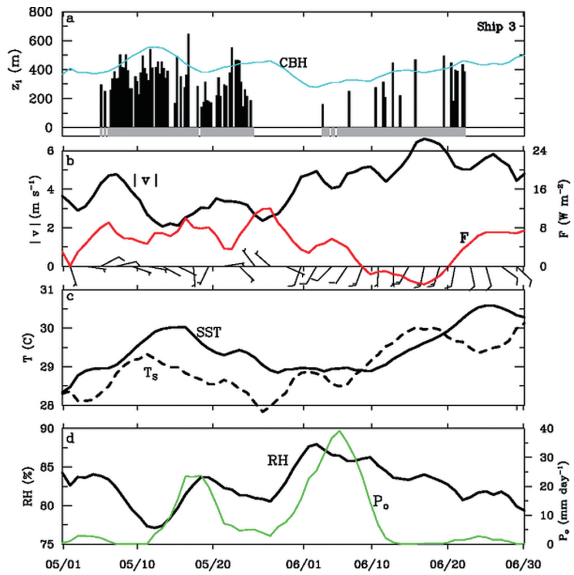

Fig. 5. As in Fig. 4, except for Ship 3.

1° gridded dataset. The procedures for adjusting the fluxes and creating the gridded dataset are described in Johnson and Ciesielski (2002). Notably, JMA fluxes collocated to those observed at Ship 3 were ~80 W m^{-2} higher than those observed in the post-onset period. The shading at the bottom of Figs. 4a and 5a indicates when the ships were on location and had successful sonde launches. The parameter CBH in meters is computed as $CBH = 125*(T_s - T_d)$ from Stull (1995, p. 88), where T_d is the surface dew point temperature. The monsoon onset, as determined by a shift in the low-level winds (Wang et al. 2004 used 850 hPa winds) from easterly to south or southwesterly over the SCS, occurred around mid-May (also see wind barbs in Figs. 4b and 5b).

The time series of fields for Ship 1, with mixed layers present 83% of the time, are typical of other tropical locations as noted earlier. While surface wind speeds averaged ~25% less at Ship 1 (Figs. 4b and 5b), surface fluxes were more than double at this site compared to those observed at the Ship 3. As noted in Ciesielski and Johnson (2006), this was due to larger air-sea temperature (Fig. 4c) and moisture gradients over the southern SCS. The magnitude of the IOP-mean total surface flux ($S+E$) at Ship 1 of 112 W m^{-2} (Ciesielski and Johnson 2006) is comparable to the time-mean observed over the intensive flux array (IFA) in TOGA COARE (115 W m^{-2}, Johnson and Ciesielski 2000). Cloud bases varied between 500 and 650 m at Ship 1 with periods of heavier rain (during cruise 2) characterized by z_i extending up to CBH, which promotes cloud development as overshooting boundary layer plumes or thermals approach the lifting condensation level (LCL). Typical of other tropical regions, the surface RH field near Ship 1 varied between 74 and 80% (Fig. 4d).

During its first cruise, suppressed convection (mean rain rate of 0.9 mm day^{-1}) and lighter winds were present in the vicinity of Ship 1 (Figs. 4b and 4d). Under these conditions, which were also observed in pre-westerly wind burst periods in TOGA COARE (JCC01), variability in the mixed-layer top was somewhat diminished, being affected primarily by radiatively driven diurnal effects. Cruise 1 mixed-layer tops at Ship 1 varied by 58 m (or 13%) from day to night with depths maximizing in the afternoon (14 LT) and evening (20 LT) soundings. A more detailed analysis of the diurnal cycle of the boundary layer during SCSMEX can be found in Yu et al. (2009a).

Enhanced convective activity (with a mean rain rate of 9.1 mm day^{-1}) was observed during the second cruise at Ship 1 which led to greater variability in mixed-layer tops. As seen in Fig. 4c, the SST continued to rise during this period while T_s slowly decreased likely from convective downdrafts transporting cool, dry air towards the surface. In response, surface buoyancy fluxes peaked during cruise 2 (Fig. 4b).

While the conditions at Ship 1 are more typical of other oceanic tropical regions, those at Ship 3, particularly during its second cruise, are quite anomalous (Fig. 5). Precipitation in the vicinity of Ship 3 shows two convectively active periods over the northern SCS; the first, centered around mid-May, was associated with the monsoon onset in this region, and a second period with even higher rain rates was observed in early June. Prior to the monsoon onset, clear skies and low-level easterlies resulted in warmer conditions over the northern SCS as evidenced by the ~1°C T_s rise and ~2°C SST rise (Fig. 5c). The greater SST increase resulted in a modest, positive surface buoyancy flux during this period (Fig. 5b). Immediately following the rainfall peak in mid-May, mixed-layer depths decreased dramatically for about a 5-day period. Such shallow boundary layers during periods of heavy rainfall, also noted in SCSMEX by Yu et al. (2009b), are likely related to recovering precipitation downdraft wakes in regions of convective rainfall (Young et al. 1995). The frequency of mixed layers during the first cruise of Ship 3 is 75% which is typical of other oceanic tropical regions. However, during its second cruise only 20% (15 out of 75) of the soundings showed a mixed-layer structure.

Conditions during the second cruise at Ship 3 are characterized by northward advection of warm, moist air. As one can note in Fig. 5, T_s tendencies at this location are affected by the wind direction such that

surface warming (cooling) generally occurs with southerly (northerly) flow. While the SST field continues to slowly warm, much of this period is characterized by T_s > SST (Fig. 5c). Despite the higher wind speeds during this time, the weak or reversed temperature gradient results in small or negative buoyancy fluxes (Fig. 5b) and few mixed layers. The mixed layers which formed during this period of negative F were likely a result of shear-generated turbulence, cloud-top radiative cooling, or horizontal advection of mixed layers from the upwind region. Extremely high RHs (> 85%) and low cloud bases (300–400 m) were also present throughout much of the second cruise. To our knowledge such anomalous conditions, resulting in negative buoyancy fluxes, weak vertical mixing and a lack of mixed layers, have not been observed in other oceanic subtropical regions.

To further examine the conditions leading to the absence of mixed layers at Ship 3, Fig. 6 shows the vertical profiles of wind speed and thermodynamic variables in the lower troposphere from Ship 3 soundings when no mixed-layer structures were present. In contrast to the mean mixed-layer profiles from Ship 3 in Fig. 3, the profiles in Fig. 6 show q decreasing and θ, θ_v increasing monotonically from the surface upward. In addition, these periods with no mixed layers were characterized at low levels by higher wind speeds (up to 2 m s^{-1}), twice the vertical shear, warmer temperatures (1°C) with stable lapse rates, and moister air (1–1.5 g kg^{-1}). The higher wind shear in Fig. 6 is consistent with less vertical mixing.

5. Summary and concluding remarks

High-vertical resolution soundings (305 total) from the R/V Kexue 1 and Shiyan 3 have been used to determine the properties of the atmospheric mixed layer over the South China Sea during SCSMEX. While the mixed-layer behavior (mean depth 459 m, frequency 83%) and atmospheric conditions at the southern Ship 1 were similar to those of other oceanic tropical regions, such was not the case at the northern Ship 3 (mean depth 342 m, frequency 48%). Following a period of heavy rainfall associated with the monsoon onset, and particularly during its second cruise, a warm, moist low-level southerly flow over cooler waters resulted in very small or negative surface buoyancy fluxes at Ship 3. These weak fluxes are likely the reason for the infrequent and shallow mixed layers at this site.

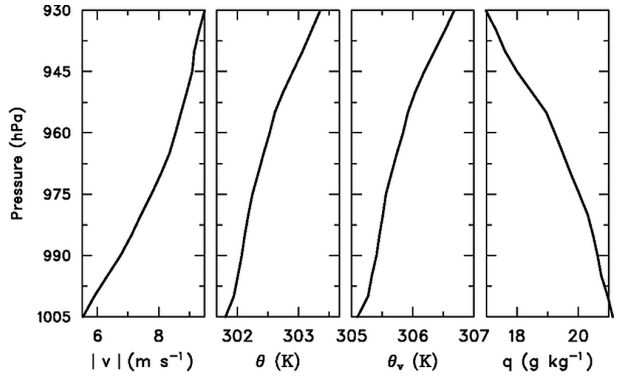

Fig. 6. Lower-troposphere mean profiles of wind speed (left panel), potential temperature (left-center panel), virtual potential temperature (right-center panel) and specific humidity (right panel) for Ship 3 when no mixed layers were present at this site.

Whether the anomalous mixed-layer features observed at Ship 3 during SCSMEX occur in other monsoon regions and seasons is uncertain. However, a preliminary examination of dropsondes and ship soundings upstream of Taiwan during TiMREX (Terrain-influenced Monsoon Rainfall Experiment) conducted in May and June, 2008 exhibited some similar features. Most notably, several soundings taken in conditions of a low-level moist southwesterly flow showed an absence of mixing in the T_d profile with moisture increasing monotonically towards the surface (C. Davis 2008 personal communication).

Finally, the large difference noted in the JMA reanalysis fluxes and those observed at Ship 3 in the post-onset period suggest that models may have difficulty in reproducing the correct boundary layer structures under weak stability conditions and may need to deal with such boundary layers differently to produce accurate predictions of lower-atmospheric variability and convection.

Acknowledgments

This research has been supported by the National Aeronautics and Space Administration (NASA) under grant NNX07AD35G. We thank Dr. Chris Davis whose early assessment of the TiMREX sonde data motivated us to undertake this study.

References

Cady-Pereira, K. E., M. W. Shephard, D. D. Turner, E. J. Mlawer, S. A. Clough, and T. J. Wagner, 2008: Improved daytime column-integrated precipitable water vapor from Vaisala radiosonde humidity sensors. *J. Atmos. Oceanic Technol.*, **25**, 873–883.

Ciesielski, P. E., and R. H. Johnson, 2006: Contrasting characteristics of convection over the Northern and Southern South China Sea during SCSMEX. *Mon. Wea. Rev.*, **134**, 1041–1062.

Fairall, C. W., E. F. Bradley, D. P. Rodgers, J. B. Edson, and G. S. Young, 1996: Bulk parameterization of air-sea fluxes for TOGA COARE. *J. Geophys. Res.*, **101**, C2, 3747–3764.

Huffman, G. J., R. F. Adler, S. Curtis, D. T. Bolvin, and E. J. Nelkin, 2007: Global rainfall analysis at monthly and 3-hr time scales. *Measuring Precipitation from Space: EURAINSAT and the Future*. V. Levizzani, P. Bauer, and J Turk, Eds., Kluwer Academic, 291–306.

Johnson, R. H., P. E. Ciesielski, and J. A. Cotturone, 2001: Multiscale variability of the atmospheric mixed layer over the Western Pacific warm pool. *J. Atmos. Sci.*, **58**, 2729–2750.

Johnson, R. H., and P. E. Ciesielski, 2002: Characteristics of the 1998 monsoon onset over the northern South China Sea. *J. Meteor. Soc. Japan*, **80**, 561–578.

Stull, R. B., 1995: Meteorology Today: *For Scientist and Engineers*. West Publishing, 385 pp.

Wang, B., L. Ho, Y. Zhang, and M.-M. Lu, 2004: Definition of the South China Sea monsoon onset and commencement of the East Asia summer monsoon. *J. Climate*, **17**, 699–710.

Wentz, F. J., C. Gentemann, D. Smith, and D. Chelton, 2000: Satellite measurements of sea surface temperature through clouds. *Science*, **288**, 847–850.

Young, G. S., S. M. Perugini, and C. W. Fairall, 1995: Convective wakes in the equatorial western Pacific during TOGA. *Mon. Wea. Rev.*, **123**, 110–123.

Yu, X., Q. Xie, and D. Wang, 2009a: The diurnal cycle of marine boundary layer during the summer monsoon over the South China Sea in 1998. *J. Tropical Ocean.*, **27**(4), (in press).

Yu, X., Q. Xie, W. Zhou, X. Wang, and D. Wang, 2009b: Characteristics of marine atmospheric boundary layer associated with the summer monsoon onset over the South China Sea in 1998. *Chinese J. Oceanol. & Limnol.*, **26**(6), (in press).

Manuscript received 2 December 2008, accepted 2 February 2009
SOLA: http://www.jstage.jst.go.jp/browse/sola/